

Published in final edited form as:

Vaccine. 2012 November 6; 30(48): 6777–6782. doi:10.1016/j.vaccine.2012.09.021.

Conjugation of *Y. pestis* F1-antigen to gold nanoparticles improves immunogenicity

A. E. Gregory¹, E. D. Williamson², J. L. Prior², W. Butcher², I. J. Thompson², A. M. Shaw¹, and R. W. Titball^{1,*}

¹Biosciences, College of Life and Environmental Sciences, University of Exeter, Devon, EX4 4QD, UK

²Defence Science and Technology Laboratory, Porton Down, SP4 0JQ, UK

Abstract

The efficacy of 15 nm gold nanoparticles (AuNP) coated with *Yersinia pestis* F1-antigen, as an immunogen in mice, has been assessed. The nanoparticles were decorated with F1-antigen using *N*-hydroxysuccinimide and 1-ethyl-3-(3-dimethylaminopropyl) carbodiimide coupling chemistry. Mice given AuNP-F1 in alhydrogel generated the greatest IgG antibody response to F1-antigen when compared with mice given AuNP-F1 in PBS or given unconjugated F1-antigen in PBS or alhydrogel. Compared with unconjugated F1-antigen, the IgG2a response was enhanced in mice dosed with AuNP-F1 in PBS ($p < 0.05$) but not in mice immunised with AuNP-F1 in alhydrogel. All treatment groups developed a memory response to F1-antigen, the polarity of which was influenced by formulation in alhydrogel. The sera raised against F1-antigen coupled to AuNPs was able to competitively bind to rF1-antigen, displacing protective macaque sera.

Keywords

Plague; *Y. pestis*; gold nanoparticle; vaccine; carbodiimide

Introduction

Yersinia pestis is a Gram-negative bacterium and the causative agent of plague [1]. Although the bacterium no longer causes pandemics of disease, the World Health Organisation estimates that world wide there are still approximately 3000 cases of plague annually [2]. The isolation of drug resistant strains, as well as the concern over the potential for *Y. pestis* to be used as a bioterrorism agent, has led to a recent resurgence in research in developing a vaccine. Immunisation with the F1-antigen, which normally encapsulates the bacterium, can provide protection against experimental plague [3–5]. Consequently, the F1-antigen is currently included in candidate plague vaccines, some of which have completed preliminary trials in humans [6–8].

The field of nanotechnology has growing applicability to medical biotechnology including drug and vaccine delivery. For example, liposomes can self-associate to form spherical

© 2012 Elsevier Ltd. All rights reserved.

*corresponding author: R.W.Titball@exeter.ac.uk, Tel (+44) 1392 725157, Fax (+44) 1392 723434.

Publisher's Disclaimer: This is a PDF file of an unedited manuscript that has been accepted for publication. As a service to our customers we are providing this early version of the manuscript. The manuscript will undergo copyediting, typesetting, and review of the resulting proof before it is published in its final citable form. Please note that during the production process errors may be discovered which could affect the content, and all legal disclaimers that apply to the journal pertain.

micelles, typically 400 nm in diameter, with an aqueous interior [9]. Polymeric micelles, made from inert materials or biodegradable polymers such as poly-L-lactide (PLA) or poly-L-lactide-co-glycolides (PLGA) allow drug encapsulation within a hydrophobic core or absorption to the hydrophilic shell. This encapsulation processes can be manipulated to encapsulate drugs or vaccines within the interior. Encapsulation technologies have allowed otherwise toxic drugs, such as paclitaxel, to be delivered without the use of toxic solvents [10].

Also of interest for drug and vaccine delivery is the use of solid NPs, composed from a range of materials and ranging in size from 1–500 nm. Some research has used gold nanoparticles (AuNPs) since they can be easily synthesised in the laboratory to provide monodisperse particles of a predetermined size [11–13]. Subsequently the rate and mechanisms of uptake of AuNPs have been determined and 50 nm particles shown to be optimal for uptake by HeLa cells [14]. Smaller particles (< 20 nm) may be able to enter mammalian cell lines via non-endosomal pathways [15, 16]. Therefore, particles of different sizes might influence the immune response to the passenger antigen. AuNPs also allow alternate immunisation routes to be used. For example, oral or nasal administration of insulin loaded AuNPs enhanced the intestinal absorption of insulin and reduced blood glucose levels in diabetic rats to a greater extent than insulin solution alone [17, 18]. AuNPs have also been used widely for the epidermal delivery of DNA vaccines using a “gene gun” [19, 20]. Despite its low delivery efficiency, this method elicits humoral and cellular immune responses making it one of the most successful approaches to DNA vaccine delivery to date [19]. Here we describe the conjugation of *Y. pestis* F1-antigen onto AuNPs, in order to determine whether this delivery system will enhance immunogenicity in mice.

2. Materials and methods

2.1 Nanoparticle synthesis

Gold(III) chloride trihydrate ($\text{HAuCl}_4 \cdot 3\text{H}_2\text{O}$, 99.9%), sodium citrate dihydrate ($\text{Na}_3\text{C}_6\text{H}_5\text{O}_7 \cdot 2\text{H}_2\text{O}$, 99%), *N*-(3-dimethylaminopropyl)-*N*'-ethylcarbodiimide hydrochloride (EDC) and *N*-hydroxysuccinimide (NHS, 98%) were purchased from Sigma-Aldrich Co. Ltd. (Gillingham, UK).

AuNPs were synthesised using the Turkevich method [13]. Briefly, 90 ml 1mM $\text{HAuCl}_4 \cdot 3\text{H}_2\text{O}$ was heated to 90°C with stirring. Next, 10 ml 90 mM $\text{Na}_3\text{C}_6\text{H}_5\text{O}_7$ was added before cooling to room temperature in the dark. Particle characterisation was carried out using ultraviolet-visible spectroscopy and their diameters determined by transmission electron microscopy (TEM).

2.2 Conjugation of protein onto gold nanoparticles

Untagged recombinant F1-antigen (rF1) was produced in *Escherichia coli* from the expression system previously described [21], under good manufacturing practice conditions. Briefly, *E. coli* harbouring the *caf* operon were grown in L-broth and centrifuged cells re-suspended in PBS to release F1-antigen from the cell surface. The F1-antigen was purified using ammonium sulphate precipitation followed by gel filtration chromatography. The F1 antigen preparation was demonstrated to be endotoxin free. The F1-antigen was immobilised onto AuNPs using carbodiimide chemistry. To a NP suspension, 0.1 mM 16-mercaptohexadecanoic acid (MHDA) was added followed by 0.1% (vol/vol) Triton®-x 100 and incubated for 2h at room temperature. The mixture was centrifuged at $13,000 \times g$ for 10 min, the supernatant removed and the pellet re-suspended in phosphate buffered saline (PBS). *N*-hydroxysuccinimide (NHS) and 1-ethyl-3-(3-dimethylaminopropyl) carbodiimide (EDC), 0.15 mM and 0.6 mM respectively were added before further adding 20 µg/ml (final

concentration) F1-antigen. The solution was incubated at room temperature for 2h. Centrifugation was used to sediment the conjugated NPs which were resuspended in PBS and characterised using spectrometry.

2.3 Protein quantification

Conjugated protein was released from AuNPs using 0.1 mM mercaptoethanol (Sigma-Aldrich), displacing the MHDA linker from the gold. The sample was separated through a NuPAGE® 4–12% Bis-Tris gel alongside known amounts of protein, before staining with Coomassie Blue. Densitometry was used to determine the amount of protein released from the AuNPs.

2.4 Immunisation

Groups of 5 female 6–8 week old BALB/c mice were immunized once with 0.1 ml per mouse by the intra-muscular (i.m.): group 1 received 0.93 µg rF1-antigen conjugated NPs formulated in 0.26% w/v alhydrogel (AuNP-F1/alhy); group 2 received 0.93 µg rF1-antigen conjugated NPs in PBS (AuNP-F1/PBS); group 3 received empty NPs in PBS (NP/PBS); group 4 received 0.93 µg rF1 formulated in 0.26% w/v alhydrogel (F1/alhy); and group 5 received 0.93 µg rF1 in PBS (F1/PBS). Mice were bled from the lateral tail vein each week to obtain blood for antibody analysis. Mice were euthanized after six weeks with terminal blood sampling and splenectomy.

2.5 Immunoanalysis

Sera from individual animals were assayed for F1-specific IgG titre using an enzyme-linked immunoassay (ELISA) [22]. Briefly, sera were aliquoted into microtitre wells pre-coated with 5 µg/ml F1 (in PBS). Binding of serum was detected using an HRP-conjugated goat anti-mouse IgG, anti-mouse IgG1 or anti-mouse IgG2a (Abcam; 1:5000 in 1% skimmed milk in TBS) followed by incubation (37°C, 1 h). ABTS substrate was added (Pierce) and the absorbance measured at 415 nm using a Multiskan plate reader. Titres were determined by comparison with a standard curve using Ascent software. Geometric mean titres were determined ± standard error of the mean for each treatment, allowing a statistical comparison of mean titres between groups, using the Student's t-test.

The detection of antibody which competed with a protective polyclonal macaque serum for binding to F1-antigen was determined as previously described [6]. Briefly, F1-antigen was coated (5 µg/ml) onto microtitre plate wells followed by the addition binding of reference serum at a 1:10 dilution. Individual sera were added in duplicate in a 2-fold dilution series in 1% (w/v) skimmed milk powder in TBS. Naive macaque serum was used as a negative control. HRP-conjugated goat anti-mouse IgG (Abcam; 1:5000 in 1% skimmed milk in TBS) was added followed by incubation (37°C, 1h). Plates were washed prior to the addition of ABTS substrate (Pierce) with subsequent reading of the absorbance at 415 nm.

2.6 Flow cytometric analysis

Spleens from individual mice were homogenised in Dulbecco's Modified Eagles Medium supplemented with L-glutamine, penicillin and streptomycin and the suspension splenocytes washed by centrifugation (10,000 rpm; 5 min) prior to collecting the cell pellet and re-suspending the cells in DMEM supplemented as described above, with additional 10% v/v foetal calf serum. Live splenocytes were enumerated and 200 µl of each was aliquoted in duplicate to the wells of a 96-well plate, and F1-antigen was added to each well at a final concentration of 25µg/ml. Plates were incubated overnight (37°C/5% CO₂). Next day, plates were centrifuged and cell culture supernatants were collected and frozen (−80°C) pending analysis of cytokines by cytometric bead assay (Becton Dickinson, UK). Non-adherent

splenocytes were removed after centrifugation, collected and stained with a mastermix of antibodies specific for surface markers CD3, CD4, CD8 and CD45, and each labelled with a different chromophore (Becton Dickinson, UK). Antibody-bound cells were analysed by fluorescence activated cells sorting (Cantifluor, Becton Dickinson, UK) and the percentage and activation status of cells in the mixed splenocyte suspension was determined.

2.6 Statistical analysis

Statistical differences between mean values were calculated using an unpaired, two-tailed Student's t-test and p values of < 0.05 were considered significant.

3. Results

3.1 Preparation of gold nanoparticles

The synthesis of AuNPs used the Turkevich method of gold chloride reduction with citrate, where the diameter of the particles was controlled by the concentration of the citrate. The particles remain stable due to the repulsion of the anionic surface in the citrate solution. Characterisation of the particles using spectrometry showed them to be monodisperse with a λ_{\max} of 519 nm (Fig. S1A). The particles were imaged using TEM and had a mean diameter of 15.6 nm (Fig. S1B). The concentration measured using NP tracking analysis was 1.37×10^8 particles/ml.

3.2 Gold nanoparticle functionalisation

In order to conjugate F1-antigen onto the NPs a linker consisting of MHDA was first bound to the NP. The MHDA was covalently attached via a gold-sulphur bond, and formed a self-assembled monolayer projecting a carboxyl group for linkage to the protein. Carboxylated NPs were purified from the bulk material, by centrifugation and washing, and then characterised by spectrophotometry, which revealed a shift in λ_{\max} from 519nm to 525 nm (Fig. S1A).

Carbodiimide coupling chemistry was used to conjugate the 15 kDa F1-antigen onto the MHDA linker. First, the concentration of F1-antigen required to saturate the NP surface was determined. Increasing concentrations of F1-antigen, in the range 0–50 $\mu\text{g/ml}$, were added to similar amounts of AuNPs. The binding of F1-antigen was assessed by monitoring the change in the wavelength of maximum absorption of visible light and also by the change in refractive index of the NPs [23]. This revealed that the NPs were saturated when 30 $\mu\text{g/ml}$ of F1-antigen was added (Fig. 1). The amount of protein conjugated onto the NPs was measured by purifying the nano-conjugates, using centrifugation and washing, and re-suspending into 2-mercaptoethanol which released the F1-antigen. The released protein was analysed in a 4–12% Bis-Tris gel stained with Coomassie blue, where the relative intensity of the protein band could be quantified against a standard curve of known concentrations (Fig. 2). The amount of protein detected using this method was 0.3 μg of protein released from 10 μl NPs, equating to approximately 160 molecules per NP.

3.2 Immunisation study

To evaluate the immunogenicity of the F1-antigen AuNP conjugated vaccine, BALB/c mice were immunised i.m. with a single dose of AuNP-F1 with or without an aluminium hydroxide adjuvant (alhydrogel). The animals were observed for six weeks and the development of antibody to F1-antigen in sera was measured using an ELISA (Fig. 3). Control mice received F1-antigen in either alhydrogel or PBS, or AuNPs alone. After 14 days, mice given AuNP-F1/alhy generated the greatest F1-antigen-specific antibody response when compared with AuNP-F1/PBS ($p < 0.01$). Mice immunised with F1/alhy generated a greater immune response than those in the groups with PBS instead of

alhydrogel ($p < 0.01$). There was a significant decline in IgG titres from mice immunised with unconjugated F1-antigen with or without alhydrogel from days 35 or 21 days respectively, post immunisation ($p < 0.01$). Mice given AuNP-F1/alhy showed no decline in IgG titre at 42 days post-immunisation. Mice immunised with empty AuNPs alone did not develop antibody against F1-antigen (data not shown). In all of the immunised groups the concentration of F1-specific IgG1 exceeded IgG2a (Table 1). However, the concentration of F1-specific IgG2a in mice immunised with AuNP-F1/PBS was significantly increased compared with mice administered unconjugated F1/PBS ($p < 0.05$). Formulation of AuNP-F1/alhy significantly increased both IgG1 and IgG2a responses, ($p < 0.01$ and $p < 0.05$, respectively), compared with AuNP-F1/PBS.

Sera collected from mice in individual treatment groups were assessed for their abilities to compete with sera from macaques previously immunised with F1-antigen. This sera has been shown to passively protect mice from a *Y. pestis* challenge [24]. The sera from mice immunised with F1-antigen formulations was able to displace the macaque sera (Fig. 4). Sera from animals immunised with AuNP-F1/alhy competed most successfully with the macaque antibody, with a significantly greater percentage bind than any other group for the initial two dilutions ($p < 0.01$). Sera from mice immunised with AuNP-F1 or unconjugated F1-antigen competed similarly with the macaque sera.

3.3 Flow cytometric analysis

Flow cytometric analysis showed that a high percentage of cells positive for the activation/maturation marker CD45 existed in all treatment groups (Table 2). CD4+ cells as a percentage of cells bearing the pan T-cell marker (CD3) exceeded CD8+ cells as a percentage of the CD3+ population, for all treatment groups, with no significant differences between groups. Analysis of IFN γ in culture supernatants of splenocytes re-stimulated *ex vivo* with F1-antigen, revealed a significantly reduced level from cells obtained from mice immunised with AuNP-F1/alhy, compared with those from mice administered F1/PBS ($P < 0.05$), indicating the anti-inflammatory influence of alhydrogel in the vaccine formulation.

4. Discussion

Previous studies have shown that i.m. immunisation with recombinant F1-antigen induces a protective immune response against *Y. pestis* [3, 5, 22]. There is also potential for a subunit vaccine composed of *Y. pestis* F1-antigen and recombinant V antigen (a secreted *Y. pestis* protein) encapsulated within polylactide microspheres to replace the current killed whole cell vaccine [22, 25]. Although promising, the immune response to this vaccine was reported to be slow to develop, attributed to the slow release of antigen from the microparticles; something which is true of many encapsulation strategies [26–28]. It would therefore be favourable to develop a delivery system which is not only self-adjuncting but induces an appropriate immune response for protection without the need for multiple dosing.

Much attention has now turned to NPs as a method for delivering vaccines [29–36]. In this study we have used F1-antigen coupled to 15 nm AuNPs. By ensuring that a non-ionic detergent, such as Triton X-100, was present during the conjugation process, we were able to separate NP-bound from free F1-antigen by centrifugation, avoiding inefficient gel chromatography steps. This method may be useful to other workers aiming to generate gold nanoconjugate vaccines.

When immunised i.m. into mice, F1 conjugated to AuNP induced antibody responses which were superior to the responses induced by F1-antigen alone. NP conjugated F1 also generated higher IgG2a titres suggesting activation of T_{h1} cells. However, IFN γ levels from splenocytes taken from mice immunised with AuNP-F1/alhy were lower than from mice

immunised with F1/PBS or with AuNP-F1/PBS. This indicates that the incorporation of alhydrogel into the formulation suppressed IFN γ responses. Unlike other studies using microspheres to deliver antigens, our data shows no delay in the induction of antibody. This is likely to be attributed to the presentation of F1-antigen on the NP surface. Similarly an attenuated strain of *Salmonella* Typhimurium expressing F1-antigen on its surface was a potent immunogen and protected mice against challenge with *Y. pestis* (24).

Other workers [37–39] have reported the ability of AuNPs to enhance the ability of antigen to evoke antibody responses compared with antigen given alone. In the case of merozoite surface protein 1 or Nogo-66 receptor, coupling to AuNPs resulted in antibody responses exceeding those elicited by the antigen given with Freund's adjuvant [38, 39]. Some workers have reported that the use of alum as an adjuvant further enhanced the responses elicited by antigen bound to AuNPs [38] but others have used antigen bound to AuNPs without an additional adjuvant [37, 39]. We found that the use of alum as an adjuvant enhanced the antibody response to F1-antigen linked to AuNPs.

F1 is a proven antigen which we know from the published literature to be immunogenic and protective against *Y. pestis* [40, 41]. Whilst we have not challenged immunised mice in this study the ability of sera from mice immunised with AuNP-F1 to compete with a protective macaque antiserum [40–42] for binding to F1-antigen indicates that the AuNP-F1 has induced a protective antibody response. Thus we conclude that the conjugation of F1-antigen to AuNPs has been successfully achieved without interference with protective B-cell epitopes in F1-antigen.

Whilst our results are encouraging, the utility of NPs as vaccine carriers requires further investigation. Gold has been used widely in medicine, but some recent publications suggest that AuNPs can accumulate within tissues and elicit toxic effects [43, 44]. These reports involve studies where high doses of NPs are repeatedly given intraperitoneally. In contrast there is also literature indicating no evidence of toxicity associated with AuNPs [39, 45] and it is possible that single doses of NPs given intramuscularly are not toxic. The toxicity of gold might also be influenced by its physical state. In the case of TiO₂ and Cu₂O, nanoparticles have been shown to be toxic inducing tissue damage and production of reactive oxygen species [44, 46–48], although larger particles lack toxicity. Further work is also required to determine the fate of AuNPs given intramuscularly and, the mechanisms by which AuNPs are taken up into antigen presenting cells requires clarification.

Supplementary Material

Refer to Web version on PubMed Central for supplementary material.

Acknowledgments

This work was partly supported by grant number U54 AI057156 from the Western Regional Center for Excellence, USA.

References

1. Evans RG, Crutcher JM, Shadel B, Clements B, Bronze MS. Terrorism from a public health perspective. *Am J Med Sci.* 2002 Jun; 323(6):291–298. [PubMed: 12074484]
2. Perry RD, Fetherston JD. *Yersinia pestis*—Etiologic Agent of Plague. *Clinical Microbiology Reviews.* 1997; 10:35–66. [PubMed: 8993858]
3. Simpson WJ, Thomas RE, Schwan TG. Recombinant capsular antigen (fraction 1) from *Yersinia pestis* induces a protective antibody response in BALB/c mice. *Am J Trop Med Hyg.* 1990 Oct; 43(4):389–396. [PubMed: 2240367]

4. Williamson ED, Eley SM, Griffin KF, Green M, Russell P, Leary SE, et al. A new improved sub-unit vaccine for plague: the basis of protection. *FEMS Immunol Med Microbiol*. 1995 Dec; 12(3–4):223–230. [PubMed: 8745007]
5. Andrews GP, Heath DG, Anderson GW Jr, Welkos SL, Friedlander AM. Fraction I capsular antigen (F1) purification from *Yersinia pestis* CO92 and from an *Escherichia coli* recombinant strain and efficacy against lethal plague challenge. *Infect Immun*. 1996 Jun; 64(6):2180–2187. [PubMed: 8675324]
6. Williamson ED, Flick-Smith HC, LeButt C, Rowland CA, Jones SM, Waters EL, et al. Human Immune Response to a Plague Vaccine Comprising Recombinant F1 and V Antigens. *Infect Immun*. 2005; 73:3598–3608. [PubMed: 15908389]
7. Fellows P, Adamovicz J, Hartings J, Sherwood R, Mega W, Brasel T, et al. Protection in mice passively immunized with serum from cynomolgus macaques and humans vaccinated with recombinant plague vaccine (rF1V). *Vaccine*. 2010; 28(49):7748–7756. [PubMed: 20920572]
8. Hart MK, Saviolakis GA, Welkos SL, House RV. Advanced Development of the rF1V and rBV A/B Vaccines: Progress and Challenges. *Advances in Preventive Medicine*. 2012; 2012:14.
9. Fahmy TM, Fong PM, Park J, Constable T, Saltzman WM. Nanosystems for simultaneous imaging and drug delivery to T cells. *Aaps J*. 2007; 9(2):E171–E180. [PubMed: 17614359]
10. Bawarski WE, Chidlowsky E, Bharali DJ, Mousa SA. Emerging nanopharmaceuticals. *Nanomedicine: Nanotechnology, Biology, and Medicine*. 2008; 4:273–282.
11. Chen S, Kimura K. Synthesis and Characterization of Carboxylate-Modified Gold Nanoparticle Powders Dispersible in Water. *Langmuir*. 1999; 15:1075–1082.
12. Chen YS, Chen SC, Kao CM, Chen YL. Effects of soil pH, temperature and water content on the growth of *Burkholderia pseudomallei*. *Folia Microbiol (Praha)*. 2003; 48(2):253–256. [PubMed: 12800512]
13. Turkevich J, Stevenson PC, Hillier J. A study of the nucleation and growth processes in the synthesis of colloidal gold. *Discuss Faraday Soc*. 1951; 11:55–75.
14. Chithrani BD, Ghazani AA, Chan WCW. Determining the Size and Shape Dependence of Gold Nanoparticle Uptake into Mammalian Cells. *Nano Letters*. 2006; 6(4):662–668. 03/01. [PubMed: 16608261]
15. Taylor U, Klein S, Petersen S, Kues W, Barcikowski S, Rath D. Nonendosomal cellular uptake of ligand-free, positively charged gold nanoparticles. *Cytometry Part A : the journal of the International Society for Analytical Cytology*. 2010 May; 77(5):439–446. [PubMed: 20104575]
16. Xia T, Rome L, Nel A. Nanobiology: Particles slip cell security. *Nat Mater*. 2008; 7(7):519–520. [PubMed: 18574478]
17. Bhumkar D, Joshi H, Sastry M, Pokharkar V. Chitosan Reduced Gold Nanoparticles as Novel Carriers for Transmucosal Delivery of Insulin. *Pharmaceutical Research*. 2007; 24(8):1415–1426. [PubMed: 17380266]
18. Pan Y, Li Y-j, Zhao H-y, Zheng J-m, Xu H, Wei G, et al. Bioadhesive polysaccharide in protein delivery system: chitosan nanoparticles improve the intestinal absorption of insulin in vivo. *Int J Pharm*. 2002; 249(1–2):139–147. [PubMed: 12433442]
19. Fuller DH, Loudon P, Schmaljohn C. Preclinical and clinical progress of particle-mediated DNA vaccines for infectious diseases. *Methods*. 2006; 40(1):86–97. [PubMed: 16997717]
20. Luo D, Saltzman WM. Synthetic DNA delivery systems. *Nat Biotech*. 2000; 18(1):33–37.
21. Miller J, Williamson ED, Lakey JH, Pearce MJ, Jones SM, Titball RW. Macromolecular organisation of recombinant *Yersinia pestis* F1 antigen and the effect of structure on immunogenicity. *FEMS Immunol Med Microbiol*. 1998 Jul; 21(3):213–221. [PubMed: 9718211]
22. Williamson DE, Sharp GJE, Eley SM, Vesey PM, Pepper TC, Titball RW, et al. Local and systemic immune response a microencapsulated sub-unit vaccine to for plague. *Vaccine*. 1996; 14:1613–1619. [PubMed: 9032889]
23. Brewer SH, Glomm WR, Johnson MC, Knag MK, Franzen S. Probing BSA Binding to Citrate-Coated Gold Nanoparticles and Surfaces. *Langmuir*. 2005; 21:9303–9307. [PubMed: 16171365]
24. Williamson ED, Packer PJ, Waters EL, Simpson AJ, Dyer D, Hartings J, et al. Recombinant (F1+V) vaccine protects cynomolgus macaques against pneumonic plague. *Vaccine*. 2011; 29(29):4771–4777. [PubMed: 21570437]

25. Quenee LE, Ciletti NA, Elli D, Hermanas TM, Schneewind O. Prevention of pneumonic plague in mice, rats, guinea pigs and non-human primates with clinical grade rV10, rV10-2 or F1-V vaccines. *Vaccine*. 2011; 29(38):6572–6583. [PubMed: 21763383]
26. Alonso MJ, Gupta RK, Min C, Siber GR, Langer R. Biodegradable microspheres as controlled-release tetanus toxoid delivery systems. *Vaccine*. 1994; 12(4):299–306. [PubMed: 8178550]
27. Alonso MJ, Cohen S, Park TG, Gupta RK, Siber GR, Langer R. Determinants of Release Rate of Tetanus Vaccine from Polyester Microspheres. *Pharmaceutical Research*. 1993; 10(7)
28. O'Hagan DT, Jeffery H, Roberts MJJ, McGee JP, Davis SS. Controlled release microparticles for vaccine development. *Vaccine*. 1991; 9(10):768–771. [PubMed: 1759495]
29. Demento SL, Cui W, Criscione JM, Stern E, Tulipan J, Kaech SM, et al. Role of sustained antigen release from nanoparticle vaccines in shaping the T cell memory phenotype. *Biomaterials*. 2012 Jun; 33(19):4957–4964. [PubMed: 22484047]
30. Musumeci T, Ventura CA, Giannone I, Ruozi B, Montenegro L, Pignatello R, et al. PLA/PLGA nanoparticles for sustained release of docetaxel. *Int J Pharm*. 2006; 325(1–2):172–179. [PubMed: 16887303]
31. Mahapatro A, Singh DK. Biodegradable nanoparticles are excellent vehicle for site directed in-vivo delivery of drugs and vaccines. *Journal of nanobiotechnology*. 2011; 9:55. [PubMed: 22123084]
32. Emeny RT, Wheeler CM, Jansen KU, Hunt WC, Fu TM, Smith JF, et al. Priming of human papillomavirus type 11-specific humoral and cellular immune responses in college-aged women with a virus-like particle vaccine. *J Virol*. 2002 Aug; 76(15):7832–7842. [PubMed: 12097595]
33. Giannini SL, Hanon E, Moris P, Van Mechelen M, Morel S, Dessy F, et al. Enhanced humoral and memory B cellular immunity using HPV16/18 L1 VLP vaccine formulated with the MPL/ aluminium salt combination (AS04) compared to aluminium salt only. *Vaccine*. 2006; 24(33–34): 5937–5949. [PubMed: 16828940]
34. Uto T, Akagi T, Hamasaki T, Akashi M, Baba M. Modulation of innate and adaptive immunity by biodegradable nanoparticles. *Immunol Lett*. 2009 Jun 30; 125(1):46–52. [PubMed: 19505507]
35. Uto T, Wang X, Sato K, Haraguchi M, Akagi T, Akashi M, et al. Targeting of antigen to dendritic cells with poly(gamma-glutamic acid) nanoparticles induces antigen-specific humoral and cellular immunity. *J Immunol*. 2007 Mar 1; 178(5):2979–2986. [PubMed: 17312143]
36. Caputoa A, Castaldello A, Brocca-Cofanoa E, Voltana R, Bortolazzi F, Altavilla G, et al. Induction of humoral and enhanced cellular immune responses by novel core-shell nanosphere- and microsphere-based vaccine formulations following systemic and mucosal administration. *Vaccine*. 2009; 27:3605–3615. [PubMed: 19464541]
37. Chen YS, Hung YC, Lin WH, Huang GS. Assessment of gold nanoparticles as a size-dependent vaccine carrier for enhancing the antibody response against synthetic foot-and-mouth disease virus peptide. *Nanotechnology*. 2010 May 14. 21(19):195101. [PubMed: 20400818]
38. Parween S, Gupta PK, Chauhan VS. Induction of humoral immune response against PfMSP-1(19) and PvMSP-1(19) using gold nanoparticles along with alum. *Vaccine*. 2011 Mar; 29(13):2451–2460. [PubMed: 21288801]
39. Wang Y-T, Lu X-M, Zhu F, Huang P, Yu Y, Zeng L, et al. The use of a gold nanoparticle-based adjuvant to improve the therapeutic efficacy of hNgR-Fc protein immunization in spinal cord-injured rats. *Biomaterials*. 2011; 32(31):7988–7998. [PubMed: 21784510]
40. Williamson ED, Eley SM, Stagg AJ, Green M, Russell P, Titball RW. A sub-unit vaccine elicits IgG in serum, spleen cell cultures and bronchial washings and protects immunized animals against pneumonic plague. *Vaccine*. 1997 Jul; 15(10):1079–1084. [PubMed: 9269050]
41. Williamson ED, Vesey PM, Gillhespy KJ, Eley SM, Green M, Titball RW. An IgG1 titre to the F1 and V antigens correlates with protection against plague in the mouse model. *Clin Exp Immunol*. 1999 Apr; 116(1):107–114. [PubMed: 10209513]
42. Williamson ED, Flick-Smith HC, Waters E, Miller J, Hodgson I, Le Butt CS, et al. Immunogenicity of the rF1+rV vaccine for plague with identification of potential immune correlates. *Microbial Pathogenesis*. 2007; 42(1):11–21. [PubMed: 17107769]

43. Abdelhalim MAK, Mady MM. Liver uptake of gold nanoparticles after intraperitoneal administration in vivo: A fluorescence study. *Lipids Health Dis.* 2011 Oct.10:9. [PubMed: 21244662]
44. Yamamoto A, Honma R, Sumita M, Hanawa T. Cytotoxicity evaluation of ceramic particles of different sizes and shapes. *Journal of biomedical materials research part A.* 2003; 68A(2):244–256.
45. Connor EE, Mwamuka J, Gole A, Murphy CJ, Wyatt MD. Gold nanoparticles are taken up by human cells but do not cause acute cytotoxicity. *Small.* 2005; 1:325–327. [PubMed: 17193451]
46. Lasagna-Reeves C, Gonzalez-Romero D, Barria MA, Olmedo I, Clos A, Sadagopa Ramanujam VM, et al. Bioaccumulation and toxicity of gold nanoparticles after repeated administration in mice. *Biochem Biophys Res Commun.* 2010 Mar 19; 393(4):649–655. [PubMed: 20153731]
47. Lovric J, Cho SJ, Winnik FM, Maysinger D. Unmodified Cadmium Telluride Quantum Dots Induce Reactive Oxygen Species Formation Leading to Multiple Organelle Damage and Cell Death. *Chemistry & Biology.* 2005; 12(11):1227–1234. [PubMed: 16298302]
48. Chen D, Zhang D, Yu JC, Chan KM. Effects of Cu2O nanoparticle and CuCl2 on zebrafish larvae and a liver cell-line. *Aquat Toxicol.* 2011 Oct; 105(3–4):344–354. [PubMed: 21839701]

Highlights

- A novel method to deliver *Y. pestis* F1-antigen using Au nanoparticles is proposed.
- Conjugation of F1-antigen to Au nanoparticles improves immunogenicity.
- F1-antigen coupled Au nanoparticles enhanced the IgG2a immune response in mice.

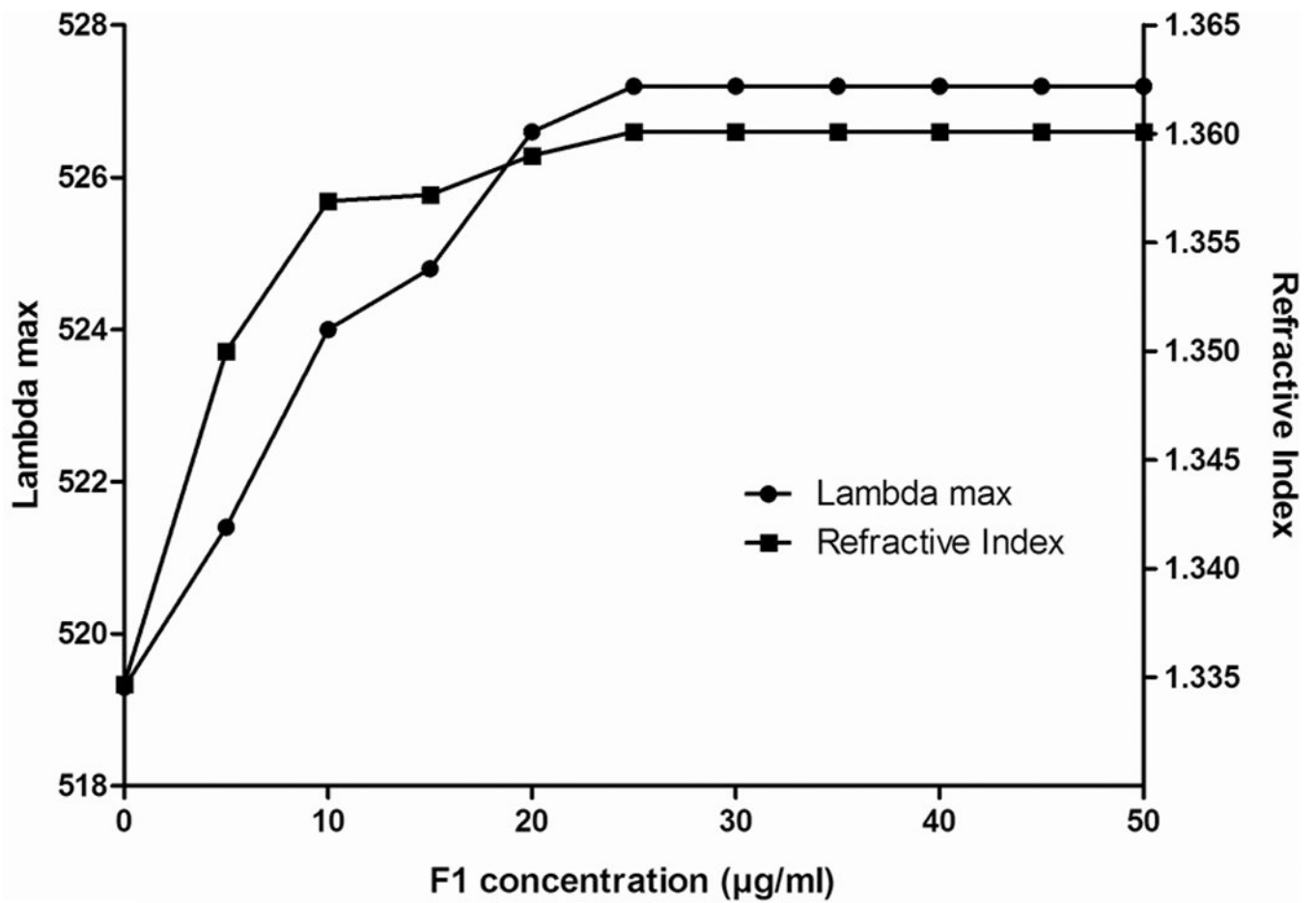


Fig. 1. Minimum protein concentrations required for AuNP saturation was determined by measuring the shift in λ_{\max} with increasing F1-antigen concentration. Graph shows a representative data set from three replicates.

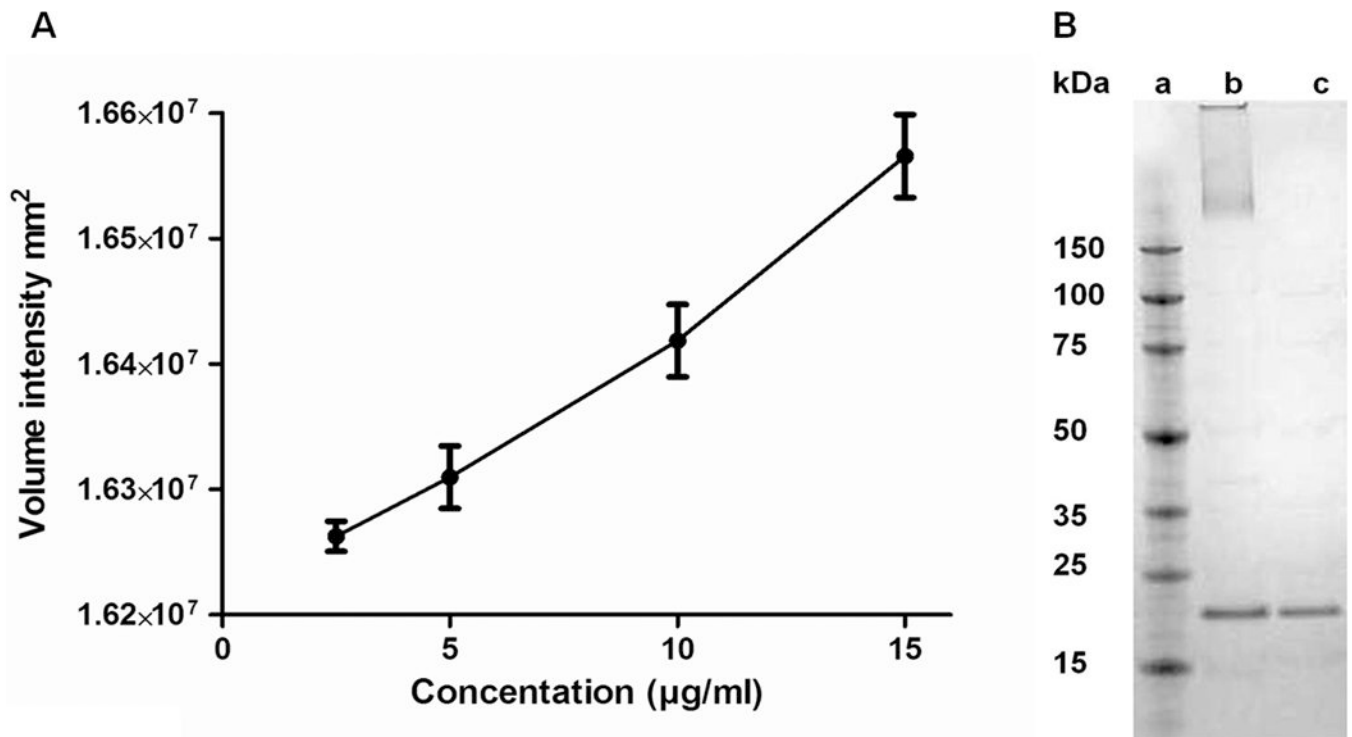


Fig. 2. Quantification of gold nanoparticle conjugated protein (A) Relationship between density of protein band from gel and concentration. A standard curve was used to calculate protein concentration released from nanoconjugate (B) Coomassie blue stained gel showing protein displacement from gold nanoparticles a: Marker, b: AuNP-F1 treated with 11-mercapto 1-undecanol (AuNP at top of lane), c: 0.2 µg F1.

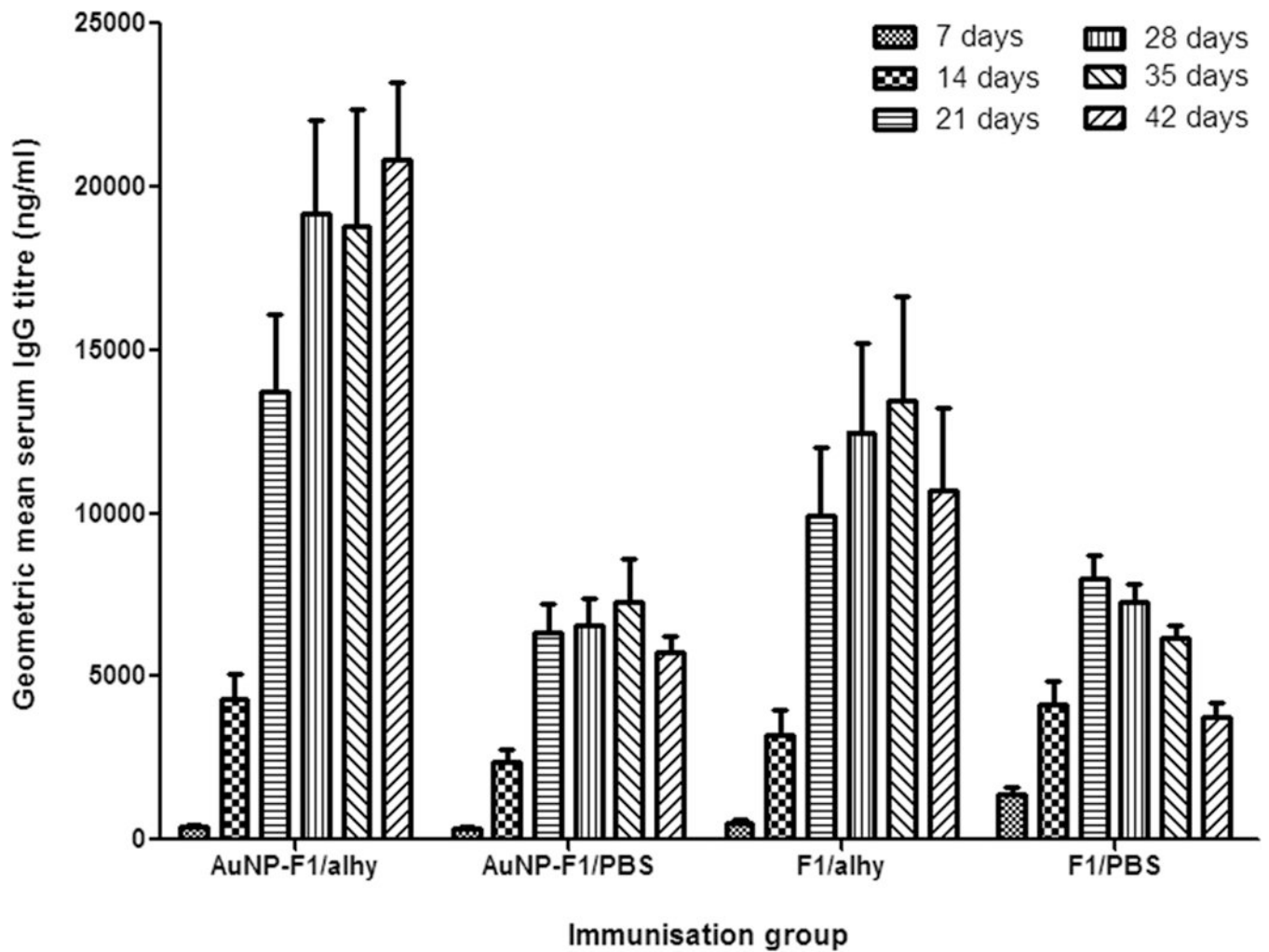


Fig. 3. Relative concentrations of F1-specific total IgG in sera from BALB/c mice at different times after giving a single dose of the immunogens indicated. After 14 days, mice immunised with gold AuNP-F1/alhy generated a significantly higher IgG titre compared with AuNP-F1/PBS or unconjugated F1-antigen in PBS ($P < 0.01$). AuNP-F1/alhy immunised mice did not show a decline in IgG at 42 days post-immunisation. Each point is the mean of values from five mice.

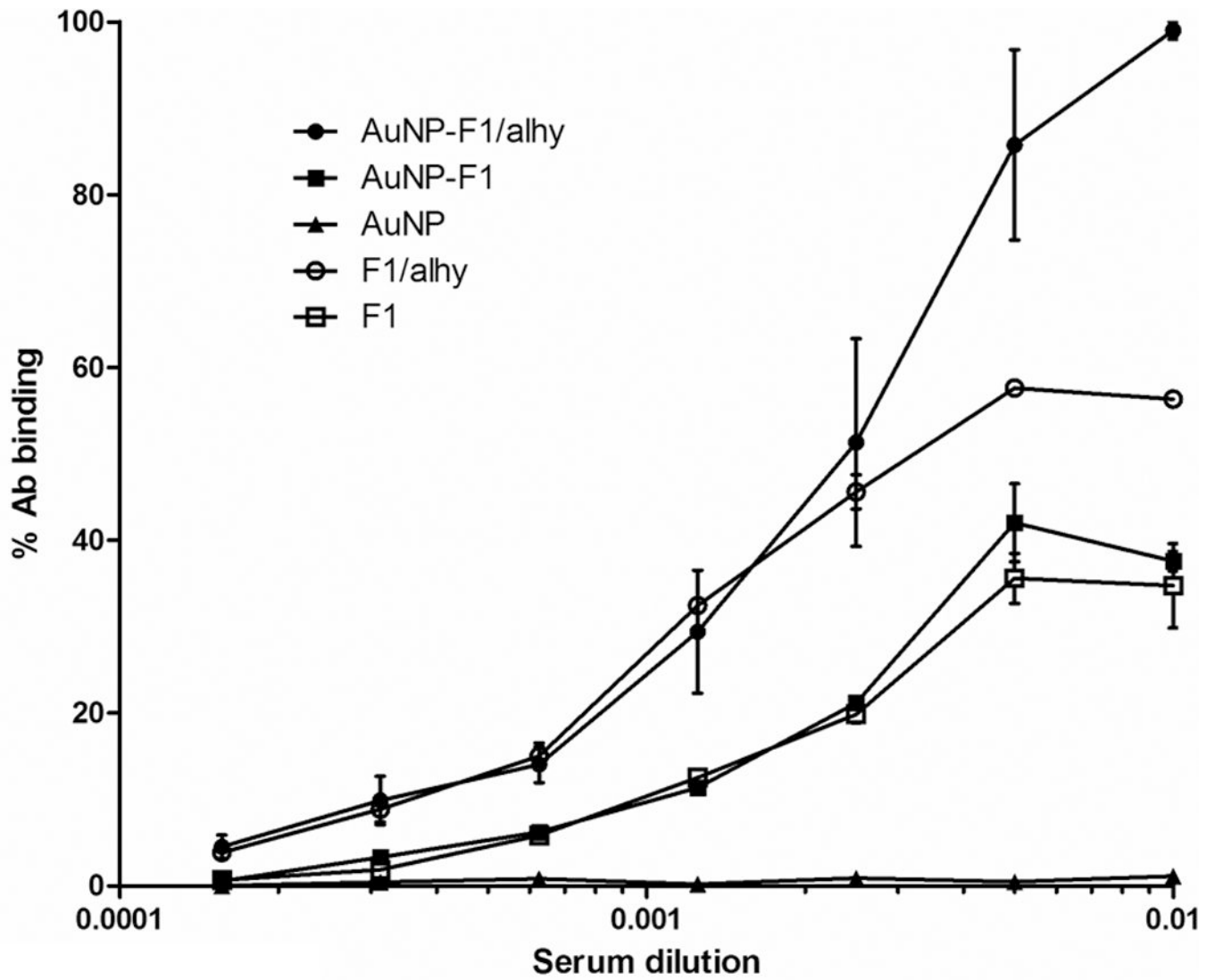


Fig. 4. Competitive ELISA for binding to F1-antigen. After 14 days, mice immunised with AuNP-F1/alhy generated a significantly higher IgG titre compared with AuNP-F1/PBS and unconjugated F1-antigen in PBS ($P < 0.01$). Mice dosed with AuNP-F1/alhy did not show a decline in total IgG at 42 days post-immunisation. Each point is the mean of values from five mice.

Table 1

Analysis of F1-specific IgG1 and IgG2a isotypes in sera taken from immunised mice. The concentration of F1-specific IgG2a in mice immunised with AuNP-F1/PBS was significantly increased compared with mice administered unconjugated F1/PBS ($p < 0.05$). Formulation of AuNP-F1/alhy significantly increased both IgG1 and IgG2a responses, ($p < 0.01$ and $p < 0.05$, respectively), compared with AuNP-F1/ PBS

Vaccine Group	IgG1 ($\mu\text{g/ml}$)	IgG2a ($\mu\text{g/ml}$)	Ratio IgG1:IgG2a
AuNP-F1/alhy	22.95 ± 3.83	1.67 ± 0.11	13.75
AuNP-F1/PBS	6.59 ± 0.86	0.98 ± 0.13	6.72
F1/alhy	12.53 ± 3.15	0.86 ± 0.18	14.57
F1/PBS	6.46 ± 0.39	0.46 ± 0.07	14.04

Table 2

Percentage of CD3⁺ splenocytes displaying the activation marker CD45 *on ex vivo* re-stimulation with F1-antigen. For all treatment groups, CD3⁺CD4⁺ cells outnumbered CD3⁺CD8⁺ cells by approximately 2:1, with no significant differences between groups. The secretion of IFN γ by restimulated splenocytes was significantly reduced in the group receiving AuNP-F1/alhydrogel, compared with the F1/PBS group ($p < 0.05$).

Vaccine group	CD45 ⁺ (% of CD3 ⁺ cells \pm s.e.m.) specifically activated by F1 <i>ex vivo</i>	IFN γ output (ng/ml \pm s.e.m.) in recall response specific for F1
AuNP-F1/alhy	89.8 \pm 2.2	327 \pm 24
AuNP-F1/PBS	86.0 \pm 5.0	704 \pm 187
F1/alhy	82.04 \pm 10.3	542 \pm 121
F1/PBS	74.8 \pm 14	775 \pm 113